ELSEVIER

Journal of Alloys and Compounds 388 (2005) 138–144

Journal of ALLOYS AND COMPOUNDS

www.elsevier.com/locate/jallcom

Study of the high temperature characteristics of hydrogen storage alloys

Rong Li*, Jianmin Wu, Yan Qi, Shaoxiong Zhou

Department of Functional Material Research, Central Iron and Steel Research Institute, 76 Xueyuan Nanlu, Haidan District, Beijing 100081, China

Received 15 May 2004; received in revised form 13 July 2004; accepted 13 July 2004

Abstract

In this work, the phase structure of as-cast and melt-spun $(MmY)_1$ $(NiCoMnAl)_5$ alloys (the content of yttrium is 0–2.5 wt.%) and their electrochemical properties were studied with regard to discharge capacity at different temperatures (30–80 °C) and cycling life at 30 °C. It is found that the substitution of yttrium increase the electrochemical capacity of the compounds and decrease the difference in capacity between as-cast and as-quenched compounds at 30 °C. When increasing the yttrium concentration from 0 to 2.5 wt.%, the cycling life of both the as-cast and the melt-spun compounds deteriorated, although the latter have a slightly longer cycle life than the former. The remarkable feature of the alloys obtained by yttrium substitution is the improvement of the high temperature electrochemical properties. It shows that the stability of the hydrides is increased. Compared with the as-cast alloys, the melt-spun ribbons have higher electrochemical charge/discharge capacity in the range of 40–80 °C, especially in the temperature range 70–80 °C. In addition, the electrochemical capacities of the melt-spun alloys showed more recovery than the as-cast alloys after charging/discharging at high temperature. This is ascribed to the better oxidation resistance. The analysis of the potential curves illustrate that the improvement of the charging/discharging efficiency for the melt-spun ribbons with yttrium substitution is ascribed to a flatter and lower hydride-formation potential as well as to a higher hydrogen evolution potential. XRD indicates that less lattice strain and defects and more anisotropy existed in melt-spun alloys. This could be beneficial to the improvement of the cycling durability and anti-corrosion properties.

Keywords: High temperature; Hydrogen storage alloy; Electrochemical properties

1. Introduction

The use of Ni/MH batteries [1] has spread quickly for consumer applications of portable electronic equipment for many years. With the development of battery technology, Ni/MH batteries have become a strong competition as power sources in the electric or hybrid-electric vehicle market because these system have high specific energy, high-power capability, inherent safety, and design flexibility [2,3]. However, other properties should be improved to answer the increased requirement for the different types of hybrid vehicles, and even for future conventional cars with 42 V electrical systems. For example, for all of batteries used in electric tools, electric or hybrid-electric vehicles (HEV), the ambient temperature might be increased to 50 °C or even to 80 °C, so the high temperature capacity of hydrogen storage alloy is also an important aspect.

The properties of hydrogen storage alloys depend on the composition as well as on the material processing. As for the commercial use of $LaNi_5$-type hydrogen storage alloys, multi-component alloying is one of the most effective methods to adjust the properties. The effect of alloying element on the performance of hydrogen storage alloy has been of interest to many researches [4–9]. Ticianelli et al. [10] studied the effect of Y as a substituent for La on the cycle life and charge/discharge reaction kinetics. It was found that the substitution of Y for La raised the equilibrium hydrogen

* Corresponding author. Tel.: +86-10-62183115; fax: +86-10-62183115.
E-mail address: cisrilee@vip.sina.com (R. Li).

0925-8388/$ – see front matter © 2004 Elsevier B.V. All rights reserved.
doi:10.1016/j.jallcom.2004.07.006

pressure of the $La_{0.6}Y_{0.4}Ni_{4.8}Mn_{0.2}$ alloy to approximately 1 MPa at room temperature [11]. Low-cobalt alloys [12–15] have also been developed due to the high price of cobalt metal. Besides, some rapid solidification techniques [16–18], namely melt-spinning, high-pressure gas atomization, etc. have proved to be effective in improving the compositional homogeneity and microstructure of hydrogen storage alloys, which will be beneficial to the durability of alloy in alkaline solution.

In this work, in order to improve the high-temperature capacity of hydrogen alloys, $(MmY)_1$ $(NiCoMnAl)_5$ low-cobalt hydrogen alloys were prepared, in which Mm (Mm denotes michmetal) was replaced by yttrium for 0, 0.5, 1.5, 2.0, 2.5 wt.%. The alloys were prepared by vacuum induction melting and followed by melt-spinning. The effect of Y as a substituent for Mm and that of melt-spinning on the phase structure and the electrochemical performance were studied systematically. The latter included capacity and cycling life, especially the effect of temperature from 30–80 °C and the recovery properties after the charge/discharge at high temperature.

2. Experimental details

All the low-cobalt alloys $(MmY)_1$ $(NiCoMnAl)_5$, where the content of yttrium is 0, 0.5, 1.5, 2.0, 2.5 wt.%, were prepared from high purity (>99.9%) starting materials by induction melting under an argon atmosphere followed by melt-spinning at a surface velocity of 22 m/s with a single copper roller, also under a purified argon atmosphere. The content of Co in all alloys is 5.0 wt.% and Mm is a natural occurring mixture of the rare earth metals, corresponding mainly to (wt.%): 62.7% La, 26.6% Ce, 7.36% Nd and 3.24% Pr. Both as-cast alloys and melt-spun ribbons were crushed and ground mechanically to produce powder below 250 mesh.

For the measurements of the electrochemical properties, approximately 1 g of alloy powder was mixed with Ni powder, in a weight ratio of 1:1, and a small amount of polyvinyl alcohol solution as a binder, and then was cold pressed to a pellet (d = 15 mm) under 20 MPa for use as the negative electrode. Electrochemical measurements were done in a three-electrode cell in 6 M KOH, with a $Ni(OH)_2$/NiOOH counter electrode and a Hg/HgO reference electrode. The capacity of the counter electrode was designed to be sufficiently large so that the capacity of the negative electrode was the limiting capacity.

In the experiment, the negative electrode was charged at 30 °C for 400 min at 60 mA/g or for 72 min at 300 mA/g current density, respectively, and after resting for 15 min, it was discharged to −0.5 V versus the Hg/HgO electrode. After resting for 2 min, it was charged again. At first, every sample was activated by subjecting it to charging/discharging at 60 mA/g current density and at 30 °C. After being activated, the test negative electrode was charged/discharged at 60 mA/g in the temperature range of 30–80 °C to determine the temperature dependence of the electrochemical properties. The cycling life experiment was carried out at 300 mA/g charge/discharge current density and at 30 °C. All the electrochemical measurement conditions and data collection were controlled and processed by a computer.

X-ray diffraction (XRD) with a $Cu_{k\alpha}$ radiation was used to characterize the phase structure of the as-cast alloys and the melt-spun ribbons. After the high temperature measurement of the alloys, the electrolyte solution was checked by ICP–AES.

3. Results and discussion

3.1. Phase structure

X-ray diffraction was used to characterize the phase structure of both as-cast and melt-spun alloys with different yttrium content. XRD patterns (Fig. 1) confirm that all of the specimens presented a single hexagonal $CaCu_5$-type structure, and no second phase was observed. It deserves to notice

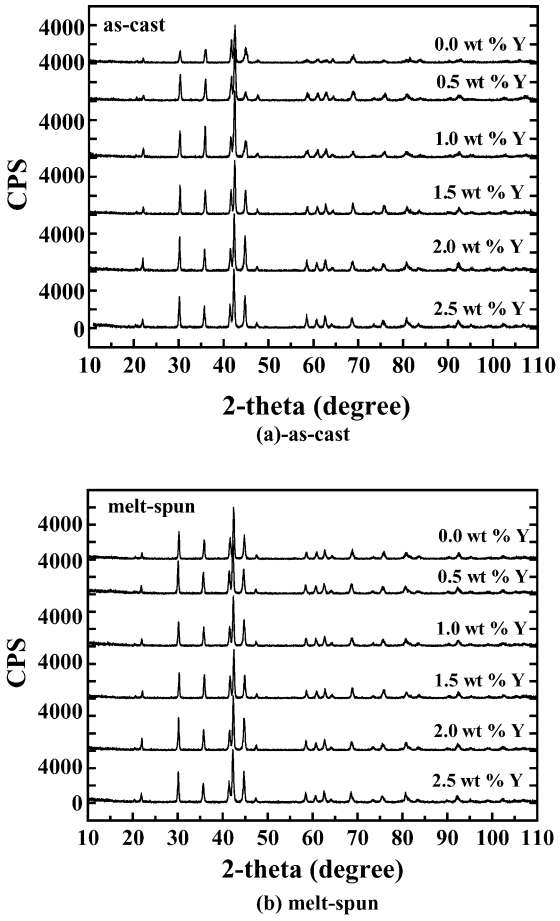

Fig. 1. The X-ray patterns of as-cast and melt-spun hydrogen storage alloys with different yttrium content.

that higher and narrower (0 0 2) peak of melt-spun ribbons indicates the existence of texture.

Different from the former research [10,11], it can be seen from Fig. 2 that the (1 1 1) and (2 0 0) peaks of the as-cast alloys and melt-spun ribbons shift to smaller angles with increasing yttrium content, implying an increase of the lattice parameters. This increase will be beneficial to lower the pressure of hydrogen absorption and desorption and increase the stability of hydride. In addition, narrower and sharper diffraction peaks were found in the melt-spun ribbons as compared with the as-cast alloys.

The full width at half-maximum (FWHM) of peak (1 1 1) is shown in Fig. 3. All of the melt-spun ribbons had a lower FWHM than the corresponding as-cast alloys. It means that the lattice strain and defects, which is introduced into the alloy during casting, are reduced [19–20]. Meanwhile, the homogenous composition of the melt-spun alloy is considered to also narrow the peak width. The FWHM values of peak (1 1 1) for all samples become gradually smaller with increasing yttrium substitution.

3.2. Capacity and cycling stability

All the specimens were first activated at 60 mA/g current density, and then the capacity and cycling stability were

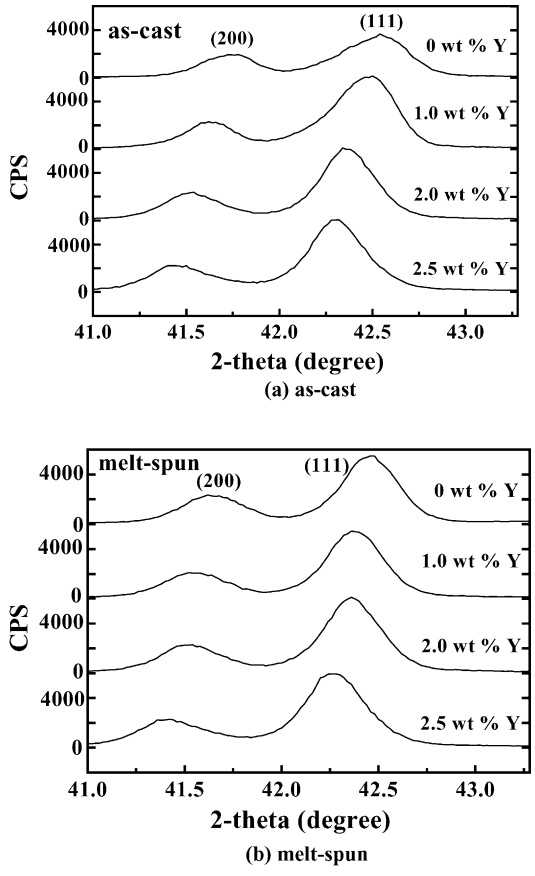

Fig. 2. Diffraction pattern of (1 1 1) and (2 0 0) peaks in as-cast alloys and melt-spun ribbons.

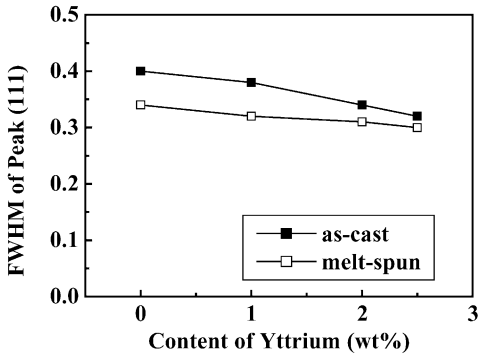

Fig. 3. The FWHM of the (1 1 1) peak in as-cast alloys and melt-spun ribbons with different yttrium content.

determined as mentioned in the experimental section. Table 1 shows the values of the maximum discharge capacity obtained for each alloy, together with the capacity retention rate with cycling. The capacity retention rate S_{200} is defined as S_{200} (%) = $C_{200}/C_{max} \times 100$, where C_{200} is the discharge capacity at the 200th cycle and C_{max} the maximum capacity when charging/discharging at 300 mA/g current density. On the whole, the capacity of the specimens increase and the cycling life decrease with the increase of the yttrium content. This result is different from a previous study [10] in which the authors reported that the cycle life of $La_{(1-x)}Y_xNi_{4.7}Sn_{0.3}$ (2.0–6.1 wt.% yttrium) improved due to reduction of the Ni corrosion in the alloys with Y, and due to the capacity decrease. Our opposite results may be attributed to the more complex effects of Mm and the lower yttrium content. The capacity increase with increasing yttrium content may have some relationship with the unit cell volume enlarging. But there is no apparent direct correlation between the cycling durability and the FWHM of the (1 1 1) peak in the different yttrium alloys.

In addition, it can be noticed that the differences in capacity between as-cast alloys and melt-spun ribbons become smaller when the yttrium content increasing from 0 to 2.0 wt.%. Compared with the as-cast alloys, a slightly better cycling stability was found in the melt-spun ribbons which is ascribed to a more homogenous composition and less lattice strain and defects.

Table 1
The capacity and cycling stability of as-cast and melt-spun hydrogen storage alloys with different yttrium content

Content of Yttrium (wt.%)	As-cast		Melt-spun	
	Capacity (mAh/g)	S_{200} (%)	Capacity (mAh/g)	S_{200} (%)
0.0	328	69.2	313	87.7
0.5	328	67.3	319	77.7
1.0	328	65.1	322	74.4
1.5	328	62.1	325	72.9
2.0	332	58.1	333	71.3
2.5	334	57.4	321	70.2

3.3. High-temperature characteristics

In this work, the effect of temperature on the electrochemical characteristics were investigated by charging/discharging the specimens at 60 mA/g current density in the temperature range of 30–80 °C. Fig. 4 displays the relationships between the temperature and capacity of both as-cast alloys and melt-spun ribbons of different yttrium content. It is the common rule that the capacity of specimens decreases when increasing the temperature from 30 to 80 °C. We found that the high-temperature capacity improves when the yttrium content increases from 0 to 2.0 wt.%, and decreases when the yttrium content reaches 2.5 wt.%. It shows that stability of hydrides increases with increasing yttrium substitution in the range of 0–2.0 wt.%.

Compared with the as-cast alloys, the melt-spun ribbons have a higher electrochemical charge/discharge capacity in the range of 40–80 °C, especially in the range of temperature 70–80 °C. Fig. 4 shows that an electrochemical capacity of more than 50 mAh/g at 70–80 °C could be obtained with melt-spun samples. In this work, an excellent capacity of 247 mAh/g was obtained at 80 °C in the melt-spun ribbons with 2.0 wt.% yttrium content.

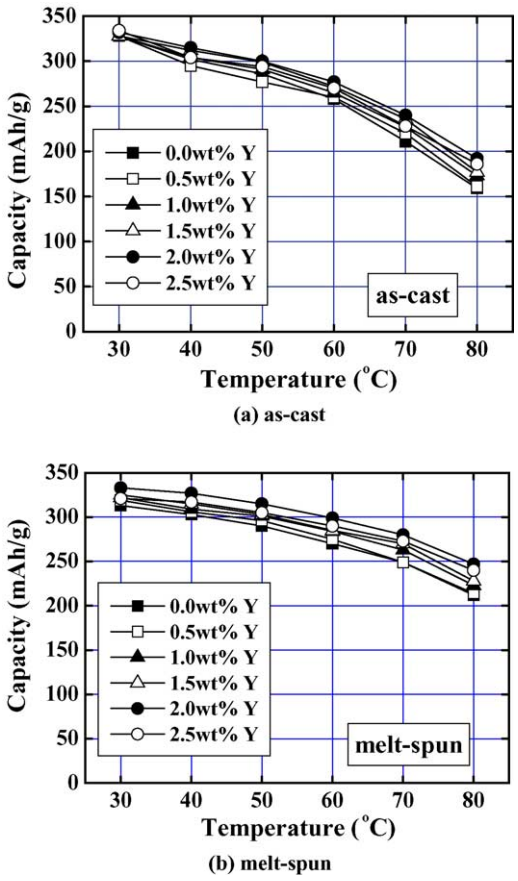

Fig. 4. The relationships between the temperature and capacity of both as-cast alloys and melt-spun ribbons with different yttrium content.

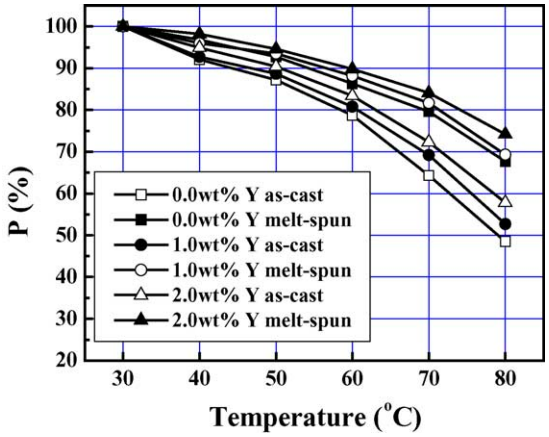

Fig. 5. The capacity retention percentage of as-cast alloys and melt-spun ribbons at different temperatures.

Fig. 5 shows the capacity retention percentage for as-cast alloys and melt-spun ribbons at different temperature. The capacity retention percentage P is defined as: P (%) = C_T/C_{30} × 100, C_T and C_{30} are the capacity at temperature of T and 30 °C, respectively. It can be found that the capacity retention percentage improves gradually for increasing yttrium content from 0 to 2.0 wt.%, and this effect becomes remarkable in melt-spun samples, especially at 70–80 °C. It is clear from Fig. 5 that the higher the temperature, the more effective is melt-spinning as to the improvement of the capacity. The capacity retention percentage can be increased from <60% in as-cast alloys to about 70% in melt-spun ribbons at 80 °C. This phenomenon indicates that the homogenous composition and less distortion and defects resulting from the melt-spinning technique could promote the corrosion resistance of the hydride at high temperature.

For power battery application, the recovery properties after charge/discharge at high temperature are more important than the high temperature properties of hydrogen storage alloy. It is because the recovery properties will affect the cycling life of the battery. In this work, the capacity of all specimens was investigated again at 30 °C after charge/discharge at the high temperature of 80 °C. Fig. 6 shows the recovery percentage of capacity of as-cast alloys and melt-spun ribbons with different yttrium content, in which the recovery percentage of the capacity denotes the rate of recovered cycle capacity to the maximum capacity present before the high temperature experiment. It can be seen that the capacity increases gradually with cycling, but it could not reach the maximum present before the high temperature experiment. Through 11 cycles the recovery percentage nearly increases up to a stable value. It means that the alloys have suffered some damage from the high temperature experiment. In addition, the favourable recovery percentage is obtained only when the content of yttrium is larger than 2.0 wt.%. Moreover, the melt-spinning technique could promote the recovery percentage from 50 to −70% in as-cast alloys to 70–85% in melt-spun ribbons. These results imply that beside the yttrium substitution, melt-

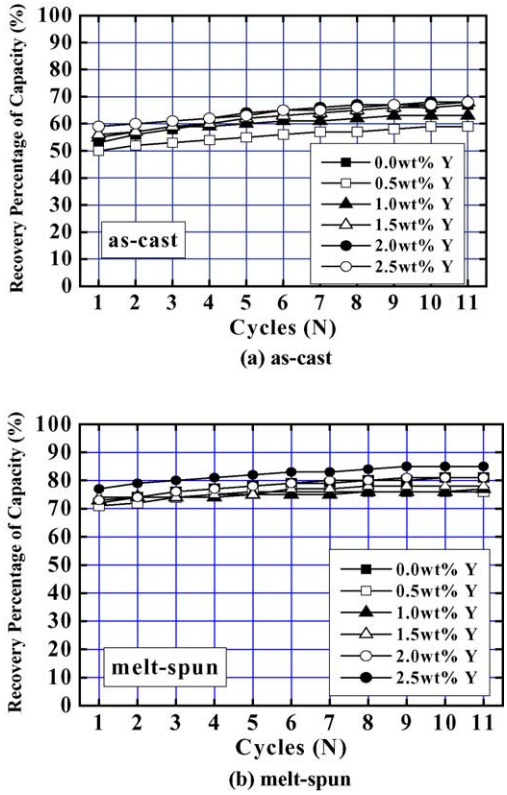

Fig. 6. The recovery percentage of capacity for as-cast alloys and melt-spun ribbons with different yttrium content.

spinning is also very important for the improvement of the anti-corrosion properties of the specimens at high temperature, especially for the recovery properties.

3.4. ICP–AES analysis of alkaline electrolyte

It is well known that some elements in AB_5-type hydrogen storage alloys are selectively dissolved into the electrolyte or forming oxides during the anodic polarization [21]. So, ICP–AES analysis of the alkaline electrolyte was carried out after the high temperature experiment. Table 2 lists the analysis results of the electrolyte used for as-cast alloys and melt-spun ribbons. For all the samples, any dissolution of ions of La, Ce, Y, Co in the electrolytes were hardly observed, the main differences are due to the dissolution of Ni, Mn and Al. Apparently, the melt-spinning technique hampers the dissolution of Ni and Mn remarkably, but still it could not avoid the dissolution of Al due to its acidity. These results reveal that the prominent cycling durability, high-temperature capacity and recovery capacity after the high temperature experiment possessed by the melt-spun ribbons come from a lower dissolution of Ni and Mn into the alkaline solution.

3.5. The potential characteristics at high temperature

It is well known that charging of a hydrogen storage electrode consists of the electrochemical reduction of water at the metal surface, resulting in the formation of absorbed hydrogen atoms. Subsequently, these hydrogen atoms diffuse into the bulk of the host metal to form a metal hydride. Discharging of such an electrode consists of dehydriding, followed by oxidation of the released hydrogen atoms. Inherent in metal hydrides both the host and the hydride are good electronic conductors. Thus, the overall electrochemical reaction is represented by the following equation:

$$AB_5 + xH_2O + xe^- \underset{\text{ch}}{\overset{\text{d}}{\Leftrightarrow}} AB_5H_x + xOH^-$$

$$E^0 = -0.86 \text{ to } -0.93 \text{ V} \quad (1)$$

Nevertheless, the recombination of two H atoms from the reduction of water has to be taken into account during the charging [22]. This leads to the formation of H_2 which is released from the electrode surface, i.e. the hydrogen evolution reaction:

$$2H_{(ad)} \rightarrow H_2 \quad (2)$$

where $H_{(ad)}$ represents the hydrogen atoms which were adsorbed chemically on the surface of the electrode. Generally, this side-reaction, (Eq. (2)), takes place after the hydride-formation reaction (Eq. (1) charging reaction), and the charge efficiency of the hydrogen storage alloy directly depends on the potential difference between the two reactions. The curves in Fig. 7 show that the hydrogen evolution potential decreases with increasing temperature, and melt-spinning could reduce this decrease. Take the example in Fig. 8, the charging/discharging potential of the melt-spun ribbons is much flatter than that of as-cast alloys, so the difference of potential between hydrogen evolution and hydride-formation is much greater, implying a higher charge efficiency. Furthermore, because there is a direct relationship between the equilibrium hydrogen pressure in a PCT curve and the electrode potential

Table 2
The ICP–AES analysis results of electrolyte for as-cast alloys and melt-spun ribbons

Yttrium content of alloys (wt.%)		Ionic concentration in electrolyte (μg/ml)						
		La	Ce	Y	Ni	Co	Mn	Al
As-cast	0.0	<0.5	<0.5	–	0.5	<0.5	0.6	20.9
	2.0	<0.5	<0.5	<0.5	0.8	<0.5	0.8	52.0
Melt-spun	0.0	<0.5	<0.5	–	<0.5	<0.5	<0.5	47.1
	2.0	<0.5	<0.5	<0.5	<0.5	<0.5	<0.5	49.1

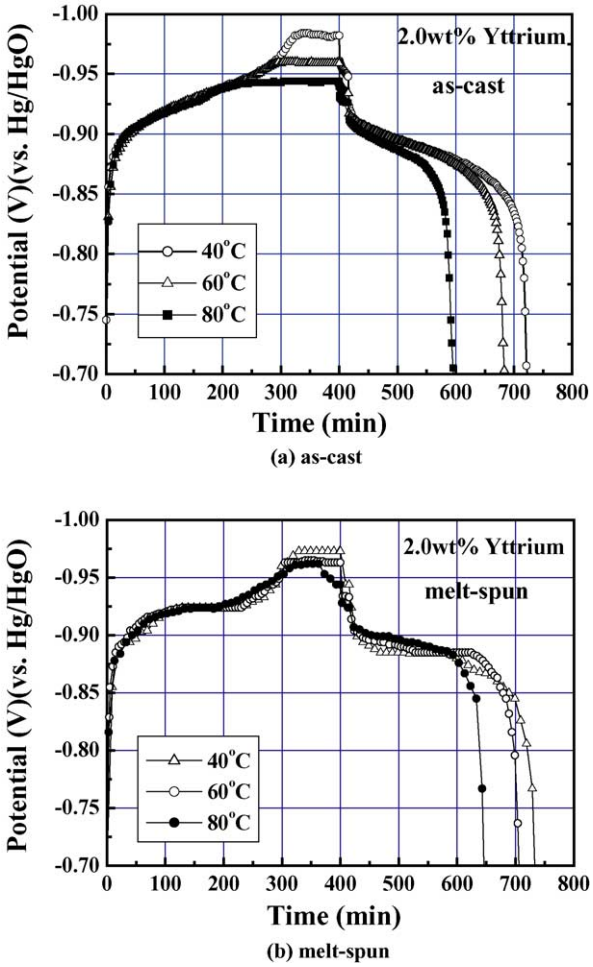

Fig. 7. The potential curves of as-cast alloy and melt-spun ribbons with 2.0 wt.% of yttrium at different temperature.

[1], flatter and lower charge potential of the melt-spun ribbons means the metal hydride stability is improved.

Fig. 9 displays the influence of yttrium content on the charging/discharging characteristics of melt-spun ribbons at

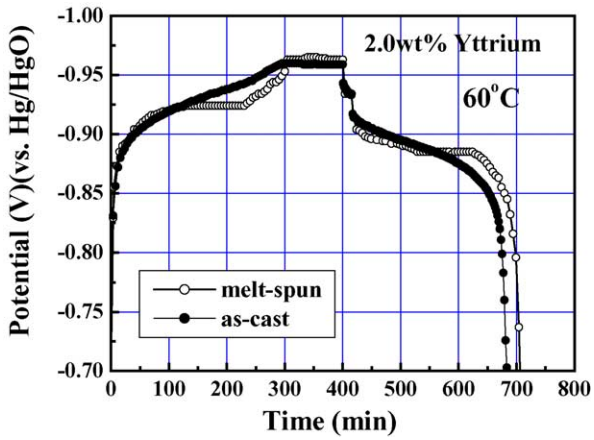

Fig. 8. A comparison of charging/discharging characteristics between as-cast and melt-spun specimens with 2.0 wt.% of yttrium at 60 °C.

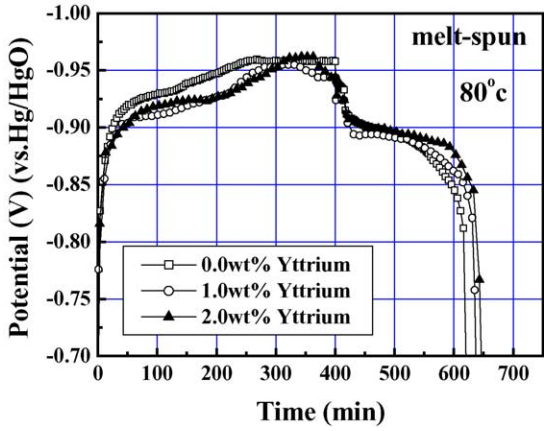

Fig. 9. A comparison of charging/discharging characteristics of melt-spun ribbons between different yttrium content at 80 °C.

80 °C. It is clear that the hydride-formation potential decreased and the hydrogen evolution reaction is postponed in yttrium-containing alloys. The flat width of the charging/discharging potential increases and the slope decrease with increasing yttrium concentration, and the hydrogen evolution potential could be increased to some extent with an appropriate yttrium content. To sum up, the improved charging/discharging efficiency for melt-spun ribbons with substitution of yttrium for Mm is ascribed to the flatter and lower hydride-formation potential as well as to the higher hydrogen evolution potential. This effect is more prominent with increasing temperature and yttrium content.

4. Conclusions

In order to improve the high-temperature characteristics of AB_5-type hydrogen storage alloys, melt-spinning and adding yttrium as a substitute for mischmetal were adopted in our work. We studied the discharge capacity at different temperatures (30–80 °C) and cycle lifetimes at 30 °C of $(MmY)_1$ $(NiCoMnAl)_5$ alloys (the content of yttrium is 0–2.5 wt.%), which were prepared by traditional casting and melt-spinning. The results obtained are as follows:

The substitution of yttrium increased the electrochemical capacity of compounds and the difference of capacity between as-cast and melt-spun compounds at 30 °C decreased. For melt-spun ribbons, the optimal capacity obtained is 333 mAh/g when the yttrium content is 2.0 wt.%.

With increasing yttrium content (0–2.5 wt.%), the cycling stability of both as-cast and melt-spun compounds deteriorates, although the latter has slightly longer life time than the former.

Compared with as-cast alloys, the melt-spun ribbons have higher electrochemical charging/discharging capacity in the range of 40–80 °C, especially in the range of 70–80 °C. The maximum capacity obtained at 80 °C is 247 mAh/g. In addition, the melt-spinning technique can promote the recovery

percentage from 50 to −70% in as-cast alloys to 70–85% in melt-spun ribbons. It shows that the melt-spun alloys have much better anti-corrosion properties.

The ICP–AES analysis of the electrolyte reveals that the dissolution of Ni and Mn into the alkaline solution can be restrained remarkably when using melt-spun alloys. So, the melt-spun ribbons possess a good cycling durability, high-temperature capacity and recovery capacity after high temperature experiment.

The potential characteristics of charging/discharging illustrate that the charging/discharging efficiency of melt-spun ribbons increases with yttrium substitution. This is ascribed to the flatter and lower hydride-formation potential as well as to the higher hydrogen evolution. Moreover, this effect becomes more prominent with increasing yttrium content.

The study of phase structure determined by XRD indicates that lattice strain and defects can be reduced and texture can be increased by the melt-spinning technique. These may be beneficial for the improvement of the cycle lifetime and the anti-corrosion properties.

Acknowledgements

This work is supported by the project (No. 2002AA323070) from National Advanced Materials Committee of China and the project (No. 50371018) provided by National Natural Science Fundation of China.

References

[1] J.J.G. Willems, Philips J. Res. 39 (1) (1984) 1.
[2] P. Gifford, J. Adams, D. Corrigan, S. Venkatesan, J. Power Sources 80 (1999) 157.
[3] K. Wiesener, D. Ohms, G. Bencaur-Urmossy, M. Berthold, E. Haschka, J. Power Sources 84 (1999) 248.
[4] F. Meli, A. Züttel, L. Schlapbach, J. Alloys Compd. 231 (1995) 639.
[5] T. Sakai, K. Oguro, H. Miyamura, N. Kuriyama, A. Kato, H. Ishikawa, C. Iwakura, J. Less-Common Met. 161 (1990) 193.
[6] G.K. Adzic, J.R. Johnson, J.J. Reilly, J. McBreen, S. Mukerjee, M.P.S. Kumar, W. Zhang, S. Srinivasan, J. Electrochem. Soc. 142 (1995) 3429.
[7] J.J.G. Willems, K.H.J. Buschow, J. Less-Common Met. 129 (1987) 13.
[8] T. Sakai, T. Hazama, H. Miyamura, N. Kuriyama, A. Kato, H. Ishikawa, J. Less-Common Met. 172–174 (1991) 1175.
[9] J.M. Cocciantelli, P. Bernard, S. Fernandez, J. Atkin, J.Alloys Compd. 253–254 (1997) 642.
[10] E.A. Ticianelli, S. Mukerjee, J. McBreen, G.D. Adzic, J.R. Johnson, J.J. Reilly, J. Electrochem. Soc. 146 (10) (1999) 3582.
[11] S. Fujitani, H. Nakamura, A. Furukawa, T. Yonesaki, K. Nasako, T. Saito, I. Yonezu, J. Alloys Compd. 192 (1993) 170.
[12] N. Higashiyama, Y. Matsuura, H. Nakamura, M. Kimoto, M. Nogami, I. Yoneau, K. Nishio, J. Alloys Compd. 253–254 (1997) 648.
[13] K. Yasuda, J. Alloys Compd. 253–254 (1997) 621.
[14] W.K. Hu, H. Lee, D.M. Kim, S.W. Jeon, J.Y. Lee, J. Alloys Compd. 268 (1998) 261.
[15] W.K. Hu, D.M. Kim, K.J. Jing, J.Y. Lee, J. Alloys Compd. 269 (1998) 254.
[16] C.J. Li, X.L. Wang, J.M. Wu, C.Y. Wang, J. Power Sources 70 (1998) 106.
[17] Yu.M. Solonin, V.V. Savin, S.M. Solonin, V.V. Skorokhod, L.L. Kolomiets, T.I. Bratanich, J. Alloys Compd. 253–254 (1997) 594.
[18] R.C. Bowman Jr., C. Witham, B. Fultz, B.V. Ratnakumar, T.W. Ellis, I.E. Anderson, J. Alloys Compd. 253–254 (1997) 613.
[19] K. Nomuram, H. Uruno, S. Ono, H. Shinozuka, S. Suda, J. Less-common Met. 107 (1985) 221.
[20] E.H. Kisi, C.E. Buckley, E.M. Gray, J. Alloys. Compd. 185 (1992) 369.
[21] F. Liu, H. Ota, S. Okamato, S. Suda, J. Alloys Compd. 253 (1997) 452.
[22] P.H.L. Notten, Rechargeable nickel–metal hydride batteries: a successful new concept, in: F. Grandjean, G.L. Long, K.H.J. Buschow (Eds.), Interstitial Intermetallic Alloys, vol. 281, Kluwer Academic Publishers, Dordrecht, 1994, pp. 151–195, NATO ASI Ser. E 281 (1995) 151.